Desalination and Water Treatment
www.deswater.com
doi: 10.1080/19443994.2014.920278

55 (2015) 637–646
July

Taylor & Francis
Taylor & Francis Group

Comparison between diffusional and first-order kinetic model, and modeling the adsorption kinetics of pyridine onto granular activated carbon

R. Leyva-Ramos, R. Ocampo-Pérez*, J.V. Flores-Cano, E. Padilla-Ortega

Facultad de Ciencias Químicas, Centro de Investigación y Estudios de Posgrado, Universidad Autónoma de San Luis Potosí, Av. Dr. M. Nava No. 6, San Luis Potosi, SLP 78210, Mexico, Tel. +52 444 813 2157; Fax: +52 444 826 2372;
emails: rlr@uaslp.mx (R. Leyva-Ramos), raul_iqi@yahoo.com.mx (R. Ocampo-Pérez), jvfc_iqi@yahoo.com.mx (J.V. Flores-Cano), aniaj_14@hotmail.com (E. Padilla-Ortega)

Received 13 November 2013; Accepted 26 April 2014

ABSTRACT

In this work, a surface diffusion model (SDM) obtained in a previous work was verified in a wide range of experimental conditions to predict the adsorption kinetics of pyridine on activated carbon. Moreover, the predictions of SDM model were compared with that obtained by using the first-order kinetic model. The results showed that the first-order model adjusted satisfactorily the experimental data. The effect of the stirring speed, mass of pyridine adsorbed, (q_e), and temperature on the rate constant of the first-order model, (k_1), was analyzed and equations were proposed to correlate k_1 as functions of q_e and temperature. Nevertheless, the dependence of k_1 regarding the temperature, stirring speed, and q_e cannot be accurately correlated, indicating that the overall adsorption rate of pyridine on activated carbon is controlled by the intraparticle diffusion. Moreover, it was shown that the rate of adsorption on active site is not controlling the overall adsorption rate. On the other hand, the SDM model provided a much better prediction than the first-order kinetic model. The surface diffusion coefficient can be readily estimated from a correlation recommended in this work, whereas the value of k_1 could not be predicted for some of the experimental conditions studied in this work.

Keywords: Activated carbon; Adsorption rate; Diffusional model; Kinetic model; Pyridine

1. Introduction

The adsorption capacity and the overall adsorption rate are required for designing fixed bed adsorbers to remove pollutants from water solutions. The overall adsorption rate on a porous solid can be described by the following consecutive steps: (i) external mass transport, (ii) intraparticle diffusion, and (iii) adsorption on an active site. Intraparticle diffusion may occur by pore volume diffusion, surface diffusion, or a combination of both mechanisms [1,2]. In general, the overall rate of adsorption may be mainly controlled by any of these mechanisms, but it is also likely that these mechanisms may be governing the overall rate of adsorption [3].

In the kinetic models, the overall rate of adsorption is assumed to be exclusively controlled by the adsorption rate of the solute on the adsorbent surface, and the intraparticle diffusion and external mass transport are fast enough to be disregarded. Moreover, it is considered that the adsorption rate of a solute on the

*Corresponding author.

surface can be represented in the same manner as the rate of a chemical reaction. In the literature, several kinetic models have been advanced to predict the adsorption rates of organic and inorganic compounds onto activated carbon. The first-order and second-order kinetic models have been widely applied to interpret the adsorption rate of many compounds on different types of porous adsorbents.

The kinetic models are very simple and easy to use and can satisfactorily interpret the rate of adsorption. It is important to point out that the shape of the experimental concentration decay curve can be easily represented with several mathematical models having two fitting constants, and this is why the kinetic models can moderately well predict the adsorption rate. The main disadvantage of the kinetic models is that their rate constants vary without any trend regarding the operating conditions such as the mass adsorbed at equilibrium, temperature, stirring speed, and particle size [4]. This behavior can drastically restrict the application of these kinetic models because they cannot be used to predict the adsorption rate. Additionally, there is no procedure for estimating the kinetic constants without fitting the experimental concentration decay data.

Unlike the kinetic models, the diffusional models take into account the mass transport mechanisms mentioned above and assumed that the adsorption rate on an active site is instantaneous. The mass transfer parameters employed to predict the adsorption rate (external mass coefficient, pore volume diffusion coefficient, and surface diffusion coefficient) can be moderately well predicted as the operating conditions are being changed.

Recently, Leyva-Ramos et al. [4] interpreted the rate of fluoride adsorption from water solution on bone char using the pore volume diffusion model (PVDM) as well as the kinetic models. The PVDM considered that the pore volume diffusion was controlling the overall rate of adsorption of fluoride. It was found that the PVDM fitted satisfactorily the experimental concentration decay curves, and the effective pore volume diffusivity of the fluoride can be estimated quite well by substituting the molecular diffusivity of fluoride and a bone char tortuosity factor of 2.1 into a relationship between the tortuosity factor and the porosity of bone char. The PVDM predicted the concentration decay curves at different experimental conditions, and the effective diffusivity of fluoride and the tortuosity factor were not dependent on the operating conditions. Additionally, the experimental concentration decay data were very well represented with the first- and second-order kinetic models. Nevertheless, the kinetic constants varied with the operating conditions without a specific trend, and no reasonable physical explanation could be advanced to argue the variation of the kinetic constants.

In a previous work, Ocampo-Perez et al. [5] investigated the overall adsorption rate of pyridine on a granular activated carbon (GAC) and observed that a diffusional model fitted very satisfactorily the concentration decay data. The results revealed that the overall rate of adsorption was controlled by intraparticle diffusion due to pore volume diffusion and surface diffusion. Furthermore, the contribution of surface diffusion to the intraparticle diffusion was more than 93.5%, confirming that the overall adsorption rate was predominantly due to surface diffusion. Additionally, the dependence of the surface diffusion coefficient on the mass of pyridine adsorbed at equilibrium, and on the temperature can be represented by Arrhenius type equations, and the surface diffusion coefficient was independent on the particle diameter.

The main aim of this work is to apply the first-order kinetic model to interpret the experimental data of the adsorption rate of pyridine onto GAC reported in the previous work [5], and to find the relationships between of kinetic constant and the operating conditions. Besides, the predictions of the diffusional model are compared to that of the kinetic model. The relationships of the rate parameters as functions of the temperature and mass of pyridine adsorbed at equilibrium would be used to predict experimental concentration decay curves of pyridine on GAC.

2. Surface diffusion model

In a previous work, it was demonstrated that the intraparticle diffusion controlled the overall adsorption rate of pyridine on GAC, and surface diffusion was the predominant intraparticle diffusion mechanism [5]. The surface diffusion model (SDM) interpreted satisfactorily well the concentration decay curves of pyridine on GAC. The following differential equations, and initial and boundary conditions represented the SDM model:

$$\mathrm{V}\frac{\mathrm{dC_A}}{\mathrm{dt}} = -\mathrm{mSk_L}\left(\mathrm{C_A} - C_A|_{r=R_p}\right) \tag{1}$$

$$t = 0 \quad C_A = C_{A0} \tag{2}$$

$$\varepsilon_p \frac{\partial C_{A,r}}{\partial t} + \rho_p \frac{\partial q}{\partial t} = \frac{1}{r^2}\frac{\partial}{\partial r}\left[r^2\left(D_S \rho_p \frac{\partial q}{\partial r}\right)\right] \tag{3}$$

$$t = 0 \quad C_{A,r} = 0 \quad 0 \le r \le R_p \tag{4}$$

$$\left.\frac{\partial C_{A,r}}{\partial r}\right|_{r=0} = 0 \tag{5}$$

$$D_S \rho_p \left.\frac{\partial q}{\partial r}\right|_{r=R_p} = k_L\left(C_A - C_A|_{r=R_p}\right) \tag{6}$$

If the adsorption rate on an active site is considered to be instantaneous, then the solute concentration in the solution within the pore is at local equilibrium with the mass of solute adsorbed on the pore surface. The following adsorption isotherm is a mathematical expression for the adsorption equilibrium:

$$q = f(C_{AR}) \tag{7}$$

The mass transport parameters of the SDM model were the external transfer coefficient (k_L) and surface diffusion coefficient (D_s). Further details of the SDM model and its numerical solution, and procedure for evaluating the mass transport parameters can be found elsewhere [5].

3. Kinetic model

3.1. First-order kinetic model

Lagergren [6] introduced the first-order kinetic model to depict the adsorption rate of oxalic and malonic acids onto charcoal. This empirical rate equation has been extensively applied to interpret the adsorption rate of solutes on different adsorbents [7–9]. The first-order kinetic model can be mathematically represented by the following equation:

$$\frac{dq}{dt} = k_1(q_e - q) \tag{8}$$

This equation can be integrated using the initial condition $q = 0$ when $t = 0$, and the preceding equation is obtained as follows:

$$q = q_e(1 - e^{-k_1 t}) \tag{9}$$

The above equation can be also expressed in terms of C_A and C_{Ae} by using the mass balance equation at a time t and equilibrium:

$$q = \frac{V(C_{A0} - C_A)}{m} \tag{10}$$

$$q_e = \frac{V(C_{A0} - C_{Ae})}{m} \tag{11}$$

These relationships can be substituted into Eq. (9), and the final equation is as follows [4]:

$$C_A = C_{Ae} + (C_{A0} - C_{Ae})e^{-k_1 t} \tag{12}$$

4. Materials and methods

4.1. Adsorbent

The GAC used in this work was manufactured from a bituminous carbon by Calgon, Inc. (Pittsburgh, PA) and is commercially traded as F-400. The GAC was sieved to an average particle diameter of 1.02 mm, washed several times with deionized water, dried in an oven set up at 393.15 K during 24 h, and stored in a plastic container.

The surface area, pore volume, average pore diameter, density of the solid, particle density, and void fraction of the GAC were $S_V = 925\ m^2/g$, $V_p = 0.534\ cm^3/g$, $d_p = 2.2$ nm, $\rho_s = 2.320\ g/cm^3$, $\rho_p = 1.036\ g/cm^3$, and $\varepsilon_p = 0.554$, respectively. Further details about the procedure for determining these properties can be found in the previous work [5].

4.2. Analysis of pyridine in water solution

The concentration of pyridine in an aqueous solution was determined by UV–Visible spectroscopy. The absorbance of a pyridine sample was measured using a double-beam spectrophotometer, Shimadzu, model UV-160, at a wavelength of 249.5 nm. The concentration of pyridine in a sample was estimated using a calibration curve (absorbance vs. concentration of pyridine), which was prepared with five standard pyridine solutions with concentrations ranging from 10 to 50 mg/L.

4.3. Method for obtaining the rate of adsorption data

A rotating basket batch adsorber was used to obtain the experimental concentration decay curves for the pyridine adsorption on GAC. This adsorber was composed of a 1 L three-neck reaction flask, and an impeller with its blades replaced with stainless steel baskets. A pyridine solution was poured into the adsorber, and the GAC particles were placed in the stainless steel mesh baskets, which were attached to a shaft connected to a variable-speed motor. The adsorber was partially immersed in a constant temperature water bath controlled by a recirculator. The procedure for obtaining the concentration decay curves of pyridine was described in much detail by Ocampo-Perez et al. [5].

The experimental data, the concentration of pyridine in the solution against time, were expressed in a dimensionless form according to the following relationship:

$$\phi_A = C_A/C_{A0} \tag{13}$$

The dimensionless concentration of pyridine, ϕ_A, was plotted against time to obtain the dimensionless concentration decay curve.

5. Results and discussion

5.1. Adsorption isotherms

In a previous work [5], it was shown that the adsorption isotherm of Prausnitz–Radke fitted satisfactorily the experimental adsorption equilibrium at pH 10 and temperatures of 288, 298, and 308 K. The equation representing this isotherm is:

$$q = \frac{aC_{Ae}}{1 + bC_{Ae}^{\beta}} \tag{14}$$

The values of the isotherm constants were reported in Table 1 of a recent paper [5]. The Prausnitz–Radke isotherm was chosen over the Langmuir and Freundlich isotherms because the Prausnitz–Radke isotherm better fitted the experimental adsorption equilibrium data than the Langmuir and Freundlich isotherms. The average percentage deviation of the Prausnitz–Radke ranged from 0.43 to 3.35%, whereas those of Langmuir and Freundlich varied from 8.41 to 11.4% and from 11.4 to 13.9%, respectively.

5.2. Interpretation of the rate of adsorption of pyridine on GAC with first-order kinetic model

The rate of adsorption of pyridine on GAC is normally represented by the dimensionless concentration decay curve of pyridine, ϕ_A vs. time. The experimental conditions for the concentration decay curves are listed in Table 1, which were reported in previous works [5,10].

The experimental concentration decay curves were interpreted with the first-order kinetic model represented by Eq. (12). The constants for the first-order kinetic model are k_1 and C_{Ae}. The value of C_{Ae} was evaluated by solving simultaneously the mass balance equation of pyridine at equilibrium, Eq. (11), and the Prausnitz–Radke adsorption isotherm, Eq. (14) [5]. The rate constant k_1 was estimated by matching the kinetic model to the experimental concentration decay curves, and the best values of this rate constant were calculated with the software Scientist, optimizing the following least-squares objective function:

$$\text{Minimum} = \sum_{1}^{N} \left(\phi_{\text{exp}} - \phi_{\text{pred}}\right)^2 \tag{15}$$

Table 1
Experimental conditions for the pyridine concentration decay curves during adsorption on GAC at pH 10 and $R_p = 0.51$ mm [5,10]

Run no.	RPM	T (K)	C_{A0} (mg/L)	m (g)	C_{Ae} (mg/L)	q_e (mg/g)	$k_1 \times 10$ (min^{-1})	%D
1	100	298.15	501.0	2.003	301.0	100.2	0.582	3.21
2	150	298.15	499.0	2.011	300.0	99.6	0.805	3.58
3	200	298.15	500.0	2.007	300.0	99.9	0.810	3.12
4	200	298.15	102.0	1.997	19.0	41.5	0.511	4.67
5	200	298.15	201.0	2.001	68.7	66.3	0.568	3.43
6	200	298.15	300.0	2.003	138.0	80.8	0.656	5.89
7	200	298.15	1011.0	2.012	753.0	129.4	1.380	6.23
8	200	298.15	499.0	1.000	392.0	108.2	0.715	3.52
9	200	298.15	499.0	2.994	226.0	91.3	1.096	5.76
10	200	298.15	499.0	4.011	166.0	83.4	1.020	4.87
11	200	298.15	499.0	5.001	117.0	76.6	0.973	3.45
12	200	288.15	499.4	2.002	294.0	102.8	0.656	4.32
13	200	288.15	300.0	2.011	122.0	88.8	0.507	3.82
14	200	288.15	100.0	1.994	16.5	41.7	0.443	3.72
15	200	308.15	499.4	2.009	307.0	96.7	0.780	5.93
16	200	308.15	304.2	2.002	149.5	77.4	0.656	4.67
17	200	308.15	100.0	1.998	19.3	40.3	0.460	6.11

The optimal values of k_1 as well as the average absolute percentage deviation are given in Table 1.

The goodness of fit of the kinetic models was evaluated estimating the average absolute percentage deviation with the subsequent equation:

$$\%D = \frac{1}{N}\sum_{i=1}^{N}\left|\frac{\phi_{\text{exp}} - \phi_{\text{pred}}}{\phi_{\text{exp}}}\right| \times 100\% \tag{16}$$

The percentage deviations ranged from 3.12 to 6.23%. These results indicated that first-order kinetic model fitted reasonably well the concentration decay curves of pyridine adsorbing on GAC. The experimental concentration decay and concentration decay predicted with the first-order kinetic model for run nos. 4–7 are plotted in Fig. 1, and it can be noticed that the kinetic model adjusted satisfactorily well the experimental data.

5.3. Effect of the operating conditions on the kinetic constant k_1

It is very well known that the rate of adsorption is dependent on the operating conditions such as the temperature, pH, stirring speed, and mass of pyridine adsorbed at equilibrium, q_e. Except for the solution pH, the effect of these conditions on k_1 was studied by performing runs keeping constant all the experimental conditions except the operating condition being studied.

The dependency of k_1 regarding the stirring speed is illustrated in Fig. 2 (Table 1, Exp. nos. 1–3). It can be observed that k_1 increased considerably when the stirring speed was increased from 100 to 150 rpm,

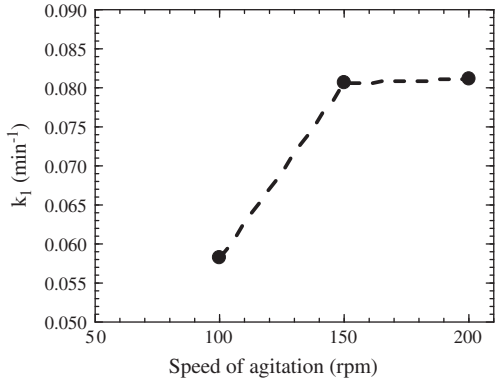

Fig. 2. Effect of the stirring speed on the kinetic constant k_1 at $T = 298.15$ K.

whereas k_1 remained almost unchanging by increasing the stirring speed from 150 to 200 rpm. This behavior is not likely since k_1 is a kinetic constant, and it cannot be dependent on the stirring speed.

The effect of the mass of pyridine adsorbed at equilibrium on k_1 is shown in Fig. 3 (Table 1, Exp. nos. 3–11) at $T = 298.15$ K. The experimental values of k_1 exhibited a large dispersion and varied without any trend as q_e was increased. This behavior cannot be explained from a theoretical basis, and k_1 cannot be properly related to q_e. However, the following linear correlation is suggested for predicting k_1:

$$k_1 = 0.0166 + 0.0008\, q_e \tag{17}$$

This correlation is plotted in Fig. 3 and can provide a very crude estimate of k_1 because the average absolute percentage deviation is $\%D = 20.2\%$. No correlation of k_1 regarding q_e was proposed at temperatures of

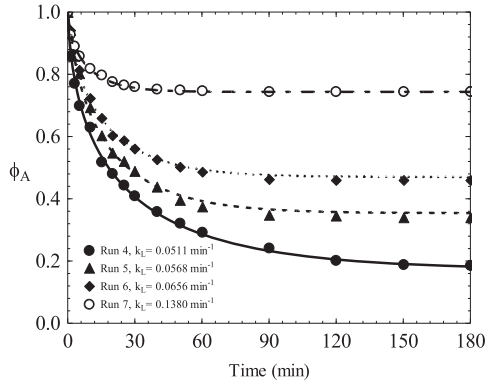

Fig. 1. Concentration decay curves for pyridine adsorption on GAC. The lines represent the predictions of first-order kinetic model.

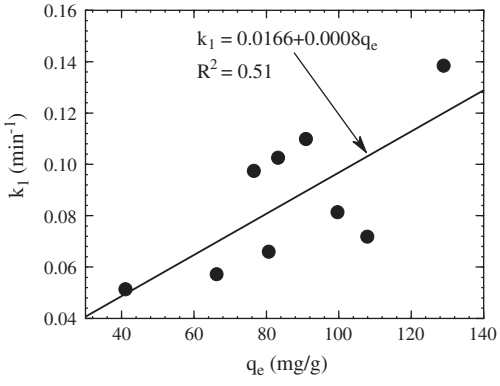

Fig. 3. Effect of the mass of pyridine adsorbed at equilibrium on the kinetic constant k_1 at $T = 298.15$ K.

Table 2
Values of the frequency factor and activation energy for k_1

Run no.	T (K)	$k_1 \times 10$ (min^{-1})	q_e (mg/g)	$\bar{q}_e$ (mg/g)	Arrhenius constants		
					A (min^{-1})	E_A (J/mol)	$\%D$
12	288.15	0.656	102.8	99.8	1.02	6490.75	5.34
3	298.15	0.810	99.9				
15	308.15	0.780	96.7				
13	288.15	0.507	88.8	82.3	2.92	9612.94	5.48
6	298.15	0.656	80.8				
16	308.15	0.656	77.4				
14	288.15	0.443	41.7	41.2	0.086	1491.72	5.43
4	298.15	0.511	41.5				
17	308.15	0.46	40.3				

288.15 and 308.15 K because the number of available data points was only 3 at each temperature.

The variation of k_1 concerning the temperature was investigated by carrying out experiments at the temperatures of 288.15, 298.15, and 308.15 K and keeping constant q_e. This last condition was required since k_1 is highly dependent upon q_e, as shown above. The values of k_1 at different temperatures are shown in Table 2 and the values of q_e at each temperature varied slightly because it was very difficult to keep constant q_e. The average values of q_e, $\bar{q}_e$, were 99.8, 82.3 and 41.2 mg/g (see Table 2) and these average values were used in the analysis of the effect of temperature. The effect of temperature on k_1 is depicted in Fig. 4 (Table 1, Exp. nos. 3, 4, 6, 12–17) and it can be noted that k_1 is strongly dependent on temperature as well as $\bar{q}_e$.

It is important to point out that k_1 has to increase by raising the temperature. This is the typical behavior of a kinetic constant regarding the temperature. The

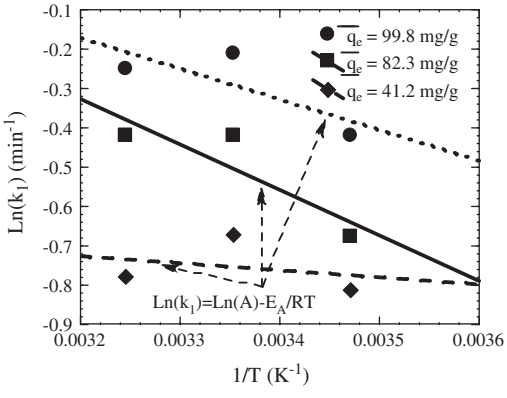

Fig. 4. Effect of the temperature on the kinetic constant k_1.

values of k_1 at $\bar{q}_e$ value of 99.8, 82.3, and 41.2 mg/g did not exhibit the proper tendency since the values of k_1 decreased, reached a minimum, and then augmented while the temperature was raised from 288.15 to 308.15 K. This last behavior is unreasonable for a kinetic constant.

At a constant q_e, the relationship between k_1 and temperature can be interpreted with the Arrhenius equation:

$$Lnk_1 = LnA - \frac{E_A}{R}\left(\frac{1}{T}\right) \tag{18}$$

where A is the pre-exponential factor and E_A is the activation energy. Eq. (18) interpreted the experimental data and the values of A and E_A are given in Table 2. The values of $\%D$ are included in Table 2 and showed that the effect of temperature on k_1 can be interpreted with the Arrhenius equation. However, the parameters A and E_A augmented, and then diminished considerably when $\bar{q}_e$ was reduced from 99.8 to 82.3 mg/g and 82.3 to 41.2 mg/g, respectively. For example, the value of A increased almost 3-folds and decreased nearly 34-folds for the above $\bar{q}_e$ ranges, correspondingly.

Eq. (18) can only be applied for the $\bar{q}_e$ values indicated in Table 3 so that the use of Eq. (18) is very limited. The above results confirm that even though the first-order kinetic model interprets the experimental data satisfactorily, k_1 cannot be properly correlated to the operating conditions and exhibited large dispersion in the correlations. Very similar results were found for the rate constant of the second-order constant [10].

The above results clearly corroborated that the kinetic constant k_1 cannot be properly correlated to the operating conditions. This behavior can be explained

Table 3
Experimental conditions for pyridine concentration decay curves during adsorption on GAC at pH 10, $m = 2.0$ g, $R = 0.51$ mm, and 200 RPM

Run no.	T (K)	C_{A0} (mg/L)	C_{Ae} (mg/L)	q_e (mg/g)	$k_L \times 10^3$ (cm/s)	$D_{s,\text{pre}} \times 10^7$ (cm^2/s)	$k_{1,\text{pred}} \times 10$ (min^{-1})
1A	298.15	430.4	246.6	91.9	8.3	2.10	0.090
2A	298.15	805.2	567.6	118.4	11.7	3.26	0.110
3A	318.15	430.4	240.9	94.4	14.9	4.70	0.100
4A	308.15	205.0	41.0	66.7	6.5	2.04	NP
5A	283.15	198.2	68.7	64.5	6.6	0.70	NP
6A	283.15	995.6	752.6	120.7	8.4	1.78	NP

NP = The value of $k_{1,\text{pred}}$ cannot be predicted with correlation (18).

by considering that the overall adsorption rate of pyridine on activated carbon is being controlled by the intraparticle diffusion instead of the adsorption rate on an active site.

Nieszporek [3] proposed a simple method to find out whether the surface reaction or the intraparticle diffusion is the rate-determining step. This method is based upon interpreting the experimental data, q vs. t, by the first-order model, Eq. (9). The full time interval is divided into few consecutive time intervals, and the value of k_1 is determined by fitting the pseudo-first-order model to the experimental data in each time interval. If k_1 is independent on the time interval, the adsorption rate is controlled by adsorption on an active site; however, if the k_1 values varied with time, the intraparticle diffusion is the rate-determining step.

The above procedure is illustrated using the kinetic data of run nos. 6 and 11 (Table 1) and the results are graphed in Fig. 5. In this figure, it can be noted that the values of k_1 for both runs are time-dependent and changed considerably. Therefore, the overall adsorption rate of pyridine on activated carbon is not controlled by the adsorption rate on an active site.

5.4. Prediction of the concentration decay curves with SDM and first-order kinetic model

The diffusional and kinetic models are normally advanced to predict the adsorption rate for designing fixed bed adsorbers to remove pollutants from an aqueous solution. Consequently, it is relevant to assess that the adsorption rate can be reliably predicted by the adsorption rate models.

Additional experimental concentration decay curves for pyridine adsorbing on GAC were obtained, and the operating conditions for all these runs are listed in Table 3. The operating conditions of these extra runs were different from those presented in Table 1. It is important to mention that the temperatures of runs nos. 3A, 5A, and 6A were outside the range, where the SDM and the first-order kinetic models were fitted to the experimental data.

In the previous work [10], the following equation was proposed to correlate the dependence of D_s as a function of q_e and T:

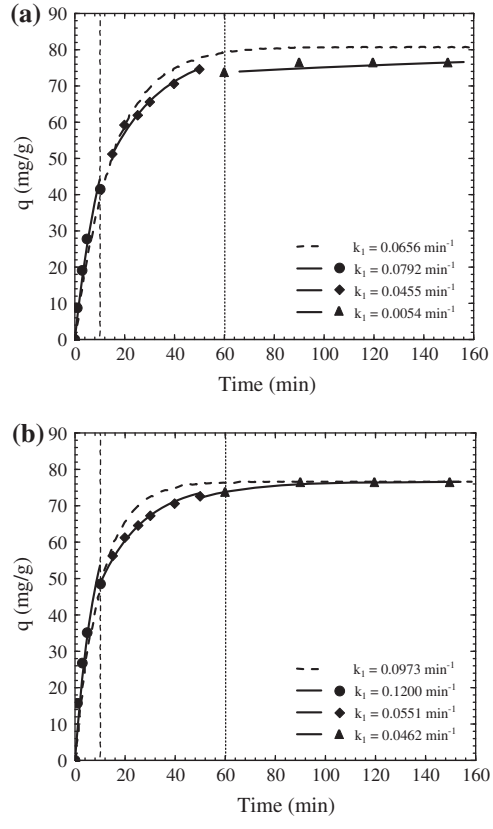

Fig. 5. The concentration decay curve of pyridine on GAC. The dashed lines are the predictions of the first-order kinetic model for a specific time range and solid line represents the prediction of the first-order kinetic model for the whole time range. Run nos. 6 and 11B.

$$D_S = D_{ST}\exp(-\alpha q_e)\exp\left(\frac{-E_S}{RT}\right) \quad (19)$$

The constants α, D_{ST}, and E_S were evaluated by a non-linear least-squares method, and the values of these constants are $\alpha = 0.0169\,\text{g/mg}$, $D_{ST} = 1.365\times10^{-2}\,\text{cm}^2/\text{s}$, and $E_S = 31.4\,\text{kJ/mol}$ [10]. The average percentage deviation of correlation (21) was estimated to be 17.9% revealing that the correlation (19) represented moderately well the dependence of D_S on the temperature and q_e.

The concentration decay curves of pyridine on GAC (Table 3, Exp. nos. 1A–6A) were predicted using the SDM model, Eqs. (1)–(7), proposed in a previous work [5] and the first-order kinetic model, Eq. (12). The parameters of these models are the surface diffusion coefficient, D_S, and the kinetic constant, k_1, and these parameters were predicted by the correlations presented in this work. As argued previously, the rate parameters D_S and k_1 are strongly dependent on the solution temperature and the mass of pyridine adsorbed at equilibrium, q_e.

The value of D_S was predicted from Eq. (19) by substituting the values of q_e and T given in Table 3. Additionally, the value of k_1 was predicted from correlations (17) and (18) presented in the Section 5.3. These values are referred to as $D_{S,\text{pred}}$ and $k_{1,\text{pred}}$, and are presented in Table 3. For runs nos. 4A–6A, it was not feasible to estimate the $k_{1,\text{pred}}$ because Eq. (18) cannot be used to interpolate or extrapolate for $\bar{q}_e$ values different from those given in Table 2. This is due to that the behavior of Eq. (18) regarding q_e and temperature does not follow a trend (see Fig. 5).

Figs. 6 and 7 depict the experimental data of the concentration decay curve for the run nos. 1A and 3A (see Table 3), correspondingly. The prediction of SDM model using $D_{S,\text{pred}}$ and first-order kinetic model with

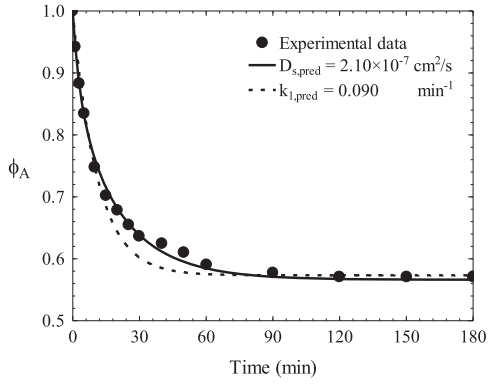

Fig. 6. The concentration decay curves predicted with the SDM and the first-order kinetic model. Run No. 1A.

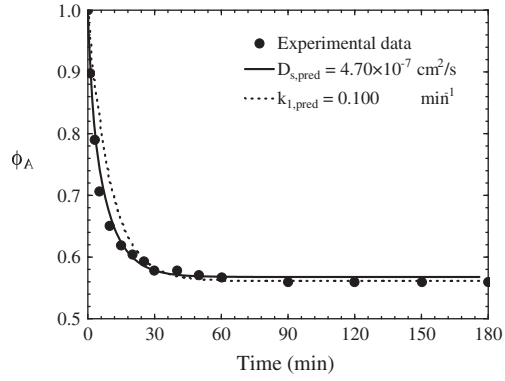

Fig. 7. The concentration decay curves predicted with the SDM and the first-order kinetic model. Run no. 3.

$k_{1,\text{pred}}$ was also graphed in Figs. 6 and 7. In both figures, it can be clearly noted that the SDM model better predicted the concentration decay data than the first-order model. Similar results were also obtained in predicting the concentration decay curve for run no. 2A. Hence, the SDM model provided much better interpretation of the rate of adsorption than the first-order model.

The concentration decay curves for run nos. 4A–6A were only predicted by the SDM model. The experimental concentration decay curve for run no. 4A and that predicted with SDM are depicted in Fig. 8. As it is shown in this figure, the SDM predicted plausibly well the experimental concentration decay curve. Similar results were observed for run nos. 5A and 6A. The values of k_1 for run nos. 4A–6A could not be predicted from correlation (18) because this correlation could only be applied for the $\bar{q}_e$ values shown in Table 2.

The above results demonstrated that D_S can be reasonably well estimated using the correlation (19).

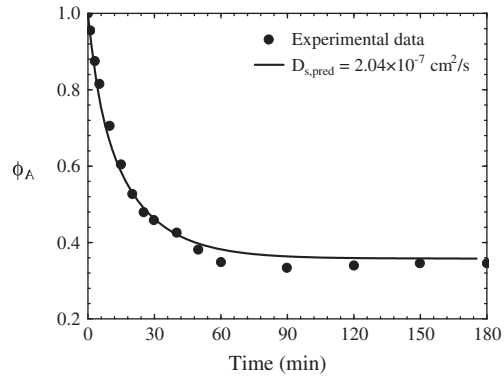

Fig. 8. The concentration decay curves predicted with the SDM. Run no. 4A.

However, the value of $k_{1,\text{pred}}$ was not feasible to predict for all the runs because the Eqs. (17) and (18) have very restricted application. This result corroborated that k_1 can be only obtained by fitting the experimental concentration decay data and thus, the application of the kinetic model is very limited.

Despite this fact, the kinetic model has been extensively used to interpret the adsorption rate because they are very simple and easy to use. However, rate constant k_1 cannot be predicted satisfactorily, restricting its application in the design of adsorption systems. On the other hand, the diffusional model is more complex to solve since it involves solving a partial and an ordinary differential equations. Moreover, it is considered that in the SDM model, the external mass transport, and especially the intraparticle diffusion play a very important role and for these reasons, it is possible to estimate their mass transport parameters in a wide range of operating conditions. Thus, the SDM model can be recommended to predict the adsorption rate of pyridine on activated carbon.

6. Conclusions

The first-order kinetic model represented reasonably well the adsorption rate of pyridine on activated carbon. However, the relationship between k_1 and the operating conditions (temperature, stirring speed, and q_e) cannot be properly correlated, even though the first-order kinetic model interpreted the experimental data satisfactorily. This result indicated that the overall adsorption rate of pyridine on GAC was not controlled by the adsorption rate on an active site, but by intraparticle diffusion.

The procedure suggested by Nieszporek [3] showed that the rate of adsorption on active site is not the rate-controlling step because the rate constant k_1 varied with time during the adsorption.

The SDM model interpreted quite well the six additional experimental concentration decay curves of pyridine using the $D_{S,\text{pred}}$. The first-order kinetic model predicted moderately only 3 of the 6 extra runs using $k_{1,\text{pred}}$ because k_1 could not be estimated from the correlations (17) and (18). This was due to that these correlations have a very limited range of application.

Acknowledgment

This work was funded by Consejo Nacional de Ciencia y Tecnologia, CONACyT, Mexico, through grant numbers INFR-2012-01-188381, CB-2012-02-182779, and MOD-ORD-12-2013PCI-0721113.

Nomenclature

a — Prausnitz–Radke isotherm constant, L/g.
A — pre-exponential factor of the kinetic constant k_1, min^{-1}.
b — Prausnitz–Radke isotherm constant, $\text{L}^{\beta}/\text{mg}^{\beta}$.
C — Concentration of pyridine at equilibrium, mg/L.
C_{A0} — initial concentration of pyridine in solution, mg/L.
C_{Ae} — final concentration of pyridine at equilibrium in solution, mg/L.
$C_{A,r}$ — concentration of pyridine in the pore volume at a distance r, mg/L.
$C_A|_{r=R_p}$ — concentration of pyridine in the solution at the external surface of GAC ($r = R_p$), mg/L.
d_p — average particle diameter of GAC, cm.
D_S — effective surface diffusivity, cm^2/s.
D_{S0} — constant of the equation for the effective surface diffusivity at constant T, cm^2/s.
D_{Sq} — constant of the equation for the effective surface diffusivity at constant q_e, cm^2/s.
D_{ST} — constant of the equation for the effective surface diffusivity, cm^2/s.
E_A — activation energy for the kinetic constant k_1, J/mol.
E_S — activation energy for the effective surface diffusivity, J/mol.
k_1 — rate constant for the first-order reaction, min^{-1}.
k_L — external mass transfer coefficient, cm/s.
m — mass of GAC, g.
N — number of experimental data.
q — mass of pyridine adsorbed per mass of GAC, mg/g.
q_e — mass of pyridine adsorbed at equilibrium per mass of GAC, mg/g.
$\bar{q}_e$ — average value of q_e, mg/g.
q_{exp} — experimental mass of pyridine adsorbed per mass of GAC, mg/g.
q_{pred} — mass of pyridine adsorbed per mass of GAC predicted with the isotherm model, mg/g.
r — distance in radial direction of GAC, cm.
R — universal gas constant, 8.314 J/mol K.
R_p — radius of the particle, cm.
S — external surface area of GAC per unit mass, cm^2/g.
t — time, s or min.
T — absolute temperature, K.
V — volume of the pyridine solution, mL or L.
V_P — pore volume per unit mass of GAC, cm^3/g.

Greek letters

α — constant for Eqs. (19) and (21), g/mg.
β — Prausnitz–Radke isotherm constant.
ε_p — void fraction of GAC.

ϕ_A — dimensionless concentration of pyridine in the solution.
ϕ_{exp} — experimental dimensionless concentration of pyridine in solution.
ϕ_{pred} — dimensionless concentration of pyridine in solution predicted with the model.
ρ_p — particle density of GAC, g/cm^3.
ρ_s — solid density of GAC, g/cm^3.

References

[1] R. Leyva-Ramos, C.J. Geankoplis, Diffusion in liquid-filled pores of activated carbon. I. Pore volume diffusion, Can. J. Chem. Eng. 72 (1994) 262–271.
[2] T.S.Y. Choong, T.N. Wong, T.G. Chuah, A. Idris, Film-pore-concentration-dependent surface diffusion model for the adsorption of dye onto palm kernel shell activated carbon, J. Colloid Interface Sci. 301 (2006) 436–440.
[3] K. Nieszporek, The balance between diffusional and surface reaction kinetic models: A theoretical study, Sep. Sci. Technol. 48 (2013) 2081–2089.
[4] R. Leyva-Ramos, J. Rivera-Utrilla, N.A. Medellin-Castillo, M. Sanchez-Polo, Kinetic modeling of fluoride adsorption from aqueous solution onto bone char, Chem. Eng. J. 158 (2010) 458–467.
[5] R. Ocampo-Perez, R. Leyva-Ramos, P. Alonso-Davila, J. Rivera-Utrilla, M. Sanchez-Polo, Modeling adsorption rate of pyridine onto granular activated carbon, Chem. Eng. J. 165 (2010) 133–141.
[6] S. Lagergren, Zur theorie der sogenannten adsorption gelöster stoffe [About the theory of so-called adsorption of soluble substances], Kungliga Svenska Vetenskapsakad emiens. Handlingar 24(4) (1898) 1–39.
[7] V.C. Srivastava, I.D. Mall, I.M. Mishra, Equilibrium modelling of single and binary adsorption of cadmium and nickel onto bagasse fly ash. Chem. Eng. J. 117(1) (2006) 79–91.
[8] C. Valderrama, X. Gamisans, X. de las Heras, A. Farran, J.L. Cortina, Sorption kinetics of polycyclic aromatic hydrocarbons removal using granular activated carbon: Intraparticle diffusion coefficients, J. Hazard. Mater. 157 (2–3) (2008) 386–396.
[9] R.L. Tseng, F.C. Wu, R.S. Juang, Characteristics and applications of the Lagergren's first-order equation for adsorption kinetics, J. Taiwan Inst. Chem. Eng. 41 (2010) 661–669.
[10] R. Ocampo-Pérez, R. Leyva-Ramos, J.V. Flores-Cano, E. Padilla-Ortega, Application of diffusional and kinetic models. Modeling the adsorption kinetics of pyridine onto granular activated carbon, Bol. Grupo Español Carbon 30 (2013) 6–9.